energies

MDPI

Article

A Hybrid-Game-Based Collaborative-Bidding and Energy-Sharing Strategy for Hydropower–Wind–Solar Virtual Power Plants Considering Multi-Market Participation and Uncertainties

Jingguang Yang [1,2], Bo Gu [1,*], Dan Wang [1], Jiawei Huang [1] and Rui Gao [1]

[1] State Key Laboratory of Advanced Electromagnetic Technology, School of Electrical and Electronic Engineering, Huazhong University of Science and Technology, Wuhan 430074, China; yang_jingguang@ctg.com.cn (J.Y.); wangdan@mail.hust.edu.cn (D.W.); jiawei_huang@hust.edu.cn (J.H.); m202472345@hust.edu.cn (R.G.)
[2] China Yangtze Power Co., Ltd. (CYPC), Yichang 443002, China
* Correspondence: gb60548@163.com

Abstract

With the increasing penetration of high-proportion renewable energy, the inherent stochasticity of wind/solar power and the volatility of electricity market prices pose significant challenges to the economic and secure operation of power systems. This paper proposes a collaborative optimization scheduling model for integrated hydropower–wind–solar virtual power plants (VPPs) based on a hybrid-game framework. The upper-level model accounts for market price uncertainty using information gap decision theory (IGDT) to construct a risk-averse decision framework, incorporating conditional value at risk (CVaR) to quantify extreme scenario risks. For the lower-level model, addressing the unknown probability distribution of renewable outputs, a data-driven distributionally robust chance-constrained (DRCC) hydropower ramping model based on Wasserstein distance is proposed. The nonlinear probabilistic constraints are reformulated into an equivalent mixed-integer linear programming (MILP) form via dual theory. Finally, a Nash bargaining mechanism is employed to ensure fair profit distribution among alliance members, solved using the alternating direction method of multipliers (ADMM) to protect agent privacy.

Keywords: optimization scheduling; hybrid game; distributionally robust chance constraint; virtual power plants; mixed-integer linear programming

Check for updates

Academic Editor: Giuseppe Marco Tina

Received: 10 July 2026
Revised: 30 September 2026
Accepted: 1 November 2026
Published: 16 November 2026

Copyright: © 2026 by the authors. Licensee MDPI, Basel, Switzerland. This article is an open access article distributed under the terms and conditions of the Creative Commons Attribution (CC BY) license.

1. Introduction

With the critical global push toward decarbonization and the mitigation of climate change, modern power systems are undergoing a rapid paradigm shift toward high-penetration renewable energy integration [1,2]. Large-scale deployment of volatile renewable sources, particularly wind power and solar photovoltaic (PV) generation, has significantly altered the supply-side dynamics of electrical grids [3]. However, the inherent stochasticity, intermittency, and non-dispatchable nature of wind and solar resources present profound operational and stability challenges to power system dispatch [4,5]. The uncoordinated injection of these volatile sources routinely exacerbates grid frequency deviations, intensifies line congestion, and increases the risk of wide-area power outages [6]. To address these challenges, the concept of the virtual power plant (VPP) has emerged as an elegant and powerful framework to aggregate geographically distributed energy

resources (DERs), controllable loads, and energy storage systems into a singular, highly flexible dispatchable entity [7–9].

Among the various flexible assets available for aggregation within a VPP portfolio, cascade hydropower stations represent an exceptional premium candidate for smoothing out renewable fluctuations [10]. Possessing massive operating capacities, zero fuel costs, and remarkably rapid ramp rates, cascade hydro units can execute highly responsive grid-balancing maneuvers [11]. Nevertheless, co-scheduling an allied portfolio of cascade hydro, wind, and solar assets introduces multi-dimensional technical complexities. From a physical standpoint, multi-stage cascade hydropower stations are bound by intricate spatiotemporal hydraulic coupling, dictated by river-routing dynamics and variable hydraulic time lags between upstream and downstream reservoirs [12,13]. Furthermore, traditional hourly scheduling intervals commonly adopted in day-ahead markets flatten intra-hour sub-hourly volatility, leaving the VPP blind to short-term ramping shortfalls [14]. Transitioning to a refined 15 min timescale is therefore paramount to explicitly capturing the exact physical ramping boundaries of hydro turbines and eliminating heavy real-time unbalance penalties imposed by grid operators [15,16]. This study notes that some ancillary markets operate on 5 min or even second-level intervals; those intervals are reserved for automatic governor response and primary frequency regulation, which are executed locally by the unit's speed-governing system rather than by the VPP day-ahead dispatch. The 15 min horizon chosen here matches the day-ahead market settlement interval and the actual ramp speed of cascade hydro units (on the order of 10–20 MW per 15 min for the stations studied), and further refinement would not tighten the ramping envelope while substantially increasing the number of variables.

Beyond the physical constraints, a practical VPP operator faces severe double-sided uncertainties: the data-driven stochasticity of wind/solar generation and the market-driven volatility of day-ahead clearing prices [17]. Historically, stochastic programming (SP) and robust optimization (RO) have been employed to handle renewable output uncertainty [18,19]. However, SP suffers from heavy computational burdens and requires predefined, precise probability distributions, whereas RO ignores probabilistic data entirely, yielding overly conservative scheduling strategies that erode profitability [20,21]. To bridge this gap, distributionally robust chance-constrained (DRCC) programming has gained immense traction [22]. By constructing an ambiguity set of probability distributions around an empirical distribution derived from historical data, the DRCC guarantees a reliable safety margin [23]. Specifically, distance-based ambiguity sets built upon the Wasserstein metric provide an optimal blend of computational tractability and structural out-of-sample performance without assuming standard error profiles [24,25]. On the market side, when historical data is insufficient to construct accurate probability distributions for price spikes or market crashes, information gap decision theory (IGDT) provides a powerful, non-probabilistic robust decision framework [26]. IGDT mathematically maps an operator's subjective risk aversion preferences onto a maximized tolerable price uncertainty radius, ensuring that a predefined baseline profit floor is tightly locked even under worst-case market price trajectories [27].

Finally, a major institutional barrier to implementing a joint hydro–wind–solar VPP lies in the conflict of economic interests among independent asset owners within the alliance [28]. While centralized optimization models maximize the collective profit of the VPP, they systematically overlook individual rationality and fair benefit reallocation, which triggers alliance instability [29]. Cooperative game theory, particularly the Nash bargaining solution, offers a mathematically sound mechanism to distribute the cooperative surplus fairly based on each participant's marginal contribution and disagreement point [30]. Given that independent asset owners prioritize data privacy regarding their internal hydraulic

operational constraints, private cost structures, and proprietary forecasting algorithms, solving this multi-member cooperative game via a centralized broker is practically unfeasible [31]. The alternating direction method of multipliers (ADMM) provides an elegant distributed optimization alternative [32]. By decoupling the subproblems of each entity, the ADMM enables the iterative clearing of internal transaction prices while strictly preserving individual data privacy, requiring only minimal information exchange regarding boundary coupling variables [33]. Similar risk-based robust strategies have also been verified in hydrogen-integrated energy systems. Ref. [34] proposed an uncertainty-aware management framework for hydrogen-powered vehicles and renewable units in microgrid transportation networks, which effectively balances operational economy and risk resilience through multi-layer risk constraints.

To comprehensively address the aforementioned physical, environmental, and institutional barriers, this paper proposes a novel bi-level hybrid-game scheduling framework for a hydro–wind–solar VPP operating at a refined 15 min resolution. The core contributions of this work are threefold:

1. A Refined 15-Minute Spatiotemporal Co-Scheduling Model: Unlike conventional 1 h scheduling paradigms, a 96-period scheduling formulation is established to explicitly capture the fast-ramping capabilities of water-linked cascade stations under precise hydraulic time lags, effectively eliminating intra-hour unbalance penalties.
2. A Bi-Level Dual-Risk Management Framework: A hybrid uncertainty-handling method is formulated where the upper level utilizes IGDT to hedge against day-ahead market price fluctuations based on risk preferences while the lower level incorporates the Wasserstein distance-based DRCC to structurally manage renewable power deviations.
3. A Privacy-Preserving Nash Bargaining Allocation: A cooperative game-theoretic mechanism is embedded to fairly reallocate the alliance surplus. A fully distributed ADMM algorithm is customized to solve the Nash bargaining problem, ensuring optimal internal trading while guaranteeing the local privacy of members' internal costs and the physical parameters for all sub-entities.

Table 1 summarizes representative recent studies on VPP uncertainty handling and cooperative clearing, highlighting the gap addressed by this work: existing studies typically address only one side of the dual uncertainty, do not combine a data-driven Wasserstein distance-based DRCC layer with an IGDT price layer, or solve the bargaining problem centrally without preserving member privacy.

Table 1. Comparison between this work and other studies.

Study	Uncertainty Handling	Cooperative/Distributed	Time Resolution	Limitation
[7]	Stochastic programming	Centralized	1 h	Needs known distribution; no price-side robustness
[19]	Robust optimization	Centralized	1 h	Over-conservative; no privacy
[24]	SP-DRCC + Stackelberg	Centralized	1 h	No IGDT layer; leader–follower but not bargaining
[27]	Wasserstein distance-based DRCC	Centralized	1 h	No price-side uncertainty and no Nash split
[32]	Two-layer game	Distributed	1 h	No dual-risk combination
This work	IGDT + CVaR + Wasserstein distance-based DRCC	Nash bargaining + ADMM	15 min (T = 96)	

The remainder of this paper is organized as follows: Section 2 establishes the mathematical modeling of the VPP elements. Section 3 delineates the bi-level hybrid-game formulation. Section 4 elaborates on the distributed ADMM-based solution methodology.

Section 5 presents the comprehensive case studies and simulation results, and Section 6 concludes the paper.

2. Hydropower–Wind–Solar VPP Architecture

2.1. VPP Composition

Figure 1 illustrates the framework of hydropower–wind–solar VPPs. The VPPs investigated in this study serve as sophisticated energy aggregators, integrating three distinct types of distributed energy resources (DERs): cascade hydropower systems, wind farms, and solar photovoltaic plants.

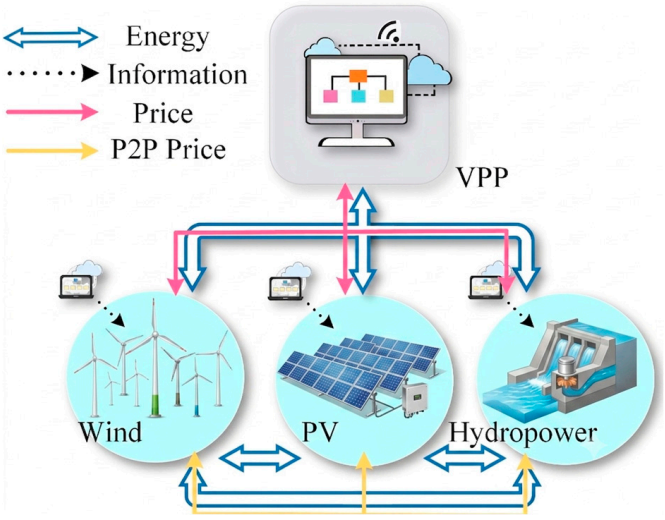


Figure 1. Hydropower–wind–solar VPP architecture.

As illustrated in Figure 1, the VPP acts as a single price-taking entity in the day-ahead, regulation and green certificate markets, while internally the hydropower, wind and solar units are linked through a peer-to-peer (P2P) energy-sharing bus: rather than each unit bidding separately and paying bilateral imbalance penalties, the aggregate internal surplus is cleared by the Nash bargaining mechanism and redistributed through an internal clearing price. This P2P internal market is the institutional core of the alliance and is what allows the cascade hydropower to serve as the flexibility buffer for the stochastic wind and solar units.

For the external integration, the VPP acts as a price-taker or strategic bidder in three concurrent markets: the day-ahead (DA) energy market, the regulation ancillary service (RAS) market, and the green electricity certificate (GEC) market. The VPP operator optimizes the aggregate bidding curve to maximize total revenue while considering the penalty costs of power imbalances.

Within the VPP, a hybrid-game framework is employed. Hydropower, characterized by its rapid response and reservoir storage, acts as the primary flexibility provider. Wind and solar units, which are stochastic providers, participate in an internal energy-sharing alliance. Hydropower prioritizes compensating for the real-time forecasting errors of the wind and solar to minimize the VPP's overall deviation penalties.

2.2. Information Flow and Market Interaction

The system operates on a hierarchical information structure. The VPP operator collects forecasted power outputs and local constraints from the DERs. It applies information gap decision theory (IGDT) to assess how much price volatility the system can withstand.

For the local resource layer, each agent maintains its own physical constraints (e.g., water head, reservoir limits, turbine efficiency). Specifically, the Wasserstein distance-based DRCC is embedded here to ensure that the hydropower's ramping capacity is reserved not just for scheduled dispatch but also as a robust buffer against renewable uncertainty.

3. Bi-Level Hybrid-Game Model Formulation

3.1. Upper Level: IGDT-CVaR Risk-Averse Model

To handle the uncertainties of market price and renewable scenarios, the objective function is formulated as a risk-augmented profit maximization: In this bi-level formulation, the VPP operator is the leader: it decides the aggregate day-ahead bidding quantities and the IGDT robustness radius (α) at the upper level, taking the risk tolerance lambda as an input. The cascade hydro, wind and solar units are the followers: they solve their own local dispatch problems under the Wasserstein distance-based DRCCs and report back their feasible operating ranges and marginal cost curves. The upper level then prices the internal P2P energy exchange through the Nash bargaining objective; this interaction is equivalent to a Stackelberg equilibrium in which the followers' optimal responses are embedded as constraints of the upper level. No iterative leader–follower loop is required because the lower-level problems are convex and their KKT conditions are substituted into the upper-level objective:

$$\max \quad \mathcal{F}_{VPP} = \sum_{t=1}^{T}\left(R_t^E + R_t^R + R_t^G - \sum_{i\in\{H,W,S\}} C_{i,t}^{oper}\right) - \beta \cdot \mathrm{CVaR}_{loss} \tag{1}$$

where R_t^E, R_t^R and R_t^G represent the revenues of the DA market, RAS market and GEC market at time (t); $C_{i,t}^{oper}$ represents the operation costs of running the hydropower, wind and solar units; β is the risk preference coefficient—a higher value indicates a more conservative operator who prioritizes safety over maximum profit. The detailed formulations are as follows:

$$R_t^E = \lambda_t^E \cdot \left[\sum_{m=1}^{M} P_{H,m,t} + P_{W,t} + P_{S,t}\right] \cdot \Delta t \tag{2}$$

$$R_t^R = \lambda_t^{up} \cdot \left(R_{H,t}^{up} + R_{W,t}^{up} + R_{S,t}^{up}\right) + \lambda_t^{dn} \cdot \left(R_{H,t}^{dn} + R_{W,t}^{dn} + R_{S,t}^{dn}\right) \tag{3}$$

$$R_t^G = \lambda_t^G \cdot \mu \cdot \left[\sum_{m\in M_{\text{small}}} P_{H,m,t} + P_{W,t} + P_{S,t}\right] \cdot \Delta t \tag{4}$$

$$\begin{aligned}\sum_{i\in\{H,W,S\}} C_{i,t}^{oper} = \sum_{m=1}^{M} (k_{H,m} \cdot P_{H,m,t} \cdot \Delta t + C_{st,m} \cdot u_{m,t}) + \\ \sum_{j\in\{W,S\}} \left[k_j \cdot P_{j,t} \cdot \Delta t + \gamma_j (R_{j,t}^{up} + R_{j,t}^{dn})\right]\end{aligned} \tag{5}$$

λ_t^E is the market clearing price at time (t). $P_{H,m,t}$ is the power output of the m-th hydropower plant in the cascade. $P_{W,t}$ and $P_{S,t}$ represent the actual power outputs of the wind and solar plants. λ_t^{up} and λ_t^{dn} represent the market prices for the upward/downward regulation capacities. $R_{i,t}^{up}$ and $R_{i,t}^{dn}$ represent the capacities reserved by unit i for regulation. λ_t^G is the price per GEC. $k_{H,m}$ is the unit maintenance cost coefficient of the m-th hydropower plant. $C_{st,m}$ is the start-up cost. While hydropower is highly flexible, frequent cycling increases mechanical degradation. k_j is the unit maintenance cost coefficient of the wind and solar plants. γ_j is the degradation coefficient for regulation.

Here, The CVaR_{loss} quantifies the expected loss in the "worst-case" scenarios of wind/solar fluctuations. We introduce an auxiliary variable (ζ) and scenario-based excess losses (η_s):

$$\mathrm{CVaR}_{loss} = \zeta + \frac{1}{1-\alpha}\sum_{s\in\delta} p_s \eta_s, \quad \text{s.t. } \eta_s \geq L_s\left(P, \tilde{\xi}_s\right) - \zeta, \eta_s \geq 0 \tag{6}$$

In the day-ahead electricity market, the volatility of clearing prices (λ_t^E) introduces significant uncertainty. Unlike stochastic optimization, which assumes a known probability distribution for price fluctuations, IGDT focuses on the robustness of the decision-making process against unknown uncertainties.

We define an uncertainty set ($U\left(\alpha, \hat{\lambda}_t^E\right)$) for the market price, where $\hat{\lambda}_t^E$ is the forecast price and α represents the uncertainty budget:

$$U\left(\alpha, \hat{\lambda}_t^E\right) = \left\{\lambda_t^E : \left|\frac{\lambda_t^E - \hat{\lambda}_t^E}{\hat{\lambda}_t^E}\right| \leq \alpha\right\}, \quad \alpha \geq 0 \tag{7}$$

The goal of the VPP operator is to maximize the robustness (α) that the system can withstand while ensuring that the total profit does not fall below a critical threshold. This is expressed as:

$$\begin{gathered} \max \alpha \\ \text{s.t. } \min_{\lambda_t^E \in U(\alpha, \lambda_t^B)} \left(\sum_{t=1}^{T} \lambda_t^E \cdot P_{VPP,t}^E \Delta t + R_t^R + R_t^G - C_t^{\text{oper}} \right) \geq (1-\delta) F_{\text{base}} \end{gathered} \tag{8}$$

where δ is the risk tolerance coefficient. It represents the percentage of the base profit the operator is willing to sacrifice to gain more robustness against price volatility.

3.2. Lower Level: Optimization Model of Hydropower–Wind–Solar Plants

The followers maximize their local utility subject to their physical and joint safety constraints. Here, the objective of the hydropower model is:

$$\max U_H = \sum_{t=1}^{T} \left(\pi_t P_{H,t}^{\text{share}} - \sum_{m=1}^{M} \left(k_{H,m} P_{H,m,t} + C_{\text{start},m} u_{m,t} \right) \right) \tag{9}$$

Hydropower is the controllable variable that can offset the randomness of wind and solar. The hydraulic coupling equation can be formulated as:

$$V_{m,t+1} = V_{m,t} + \left(I_{m,t} + \sum_{j \in \Omega_m} Q_{j,t-\tau} - Q_{m,t}^{\text{gen}} - Q_{m,t}^{\text{spill}} \right) \Delta t \tag{10}$$

where $V_{m,t}$ is the reservoir storage, $I_{m,t}$ is the natural water inflow from rain or rivers, $Q_{j,t-\tau}$ is the outflow from upstream plant j that reaches plant m after a time lag. $Q_{m,t}^{\text{gen}}$ is the water flow used for generation. The power output can be formulated as:

$$P_{H,m,t} = \eta_m \rho g H_{m,t} Q_{m,t}^{gen} \tag{11}$$

Here, $H_{m,t}$ represents the net water head. It is a function of the water level in the reservoir. To preserve the MILP tractability claimed in this paper, the turbine efficiency eta is treated not as a constant but as a piecewise-linear function of the net head and discharge, approximated from the unit's design hill chart; the piecewise-linear segments are convex and therefore do not compromise the convexity of the overall formulation:

$$H_{m,t} = c_1 V_{m,t}^2 + c_2 V_{m,t} + c_3 - d_1 \left(Q_{m,t}^{\text{out}}\right)^2 - d_2 Q_{m,t}^{\text{out}} - \Delta h_{\text{loss}} \tag{12}$$

The objective of renewable energy models is:

$$\max U_i = \sum_{t=1}^{T} \left(\pi_t P_{i,t}^{share} - k_i P_{i,t} - \gamma_i \left(R_{i,t}^{up} + R_{i,t}^{dn} \right) \right), \quad i \in \{W, S\} \tag{13}$$

Wind and solar power output are stochastic sources composed of a forecast and an error, which can be formulated as:

$$\widetilde{P}_{\text{Renew},t} = \hat{P}_{\text{Renew},t} + \Delta\tilde{\xi}_t \tag{14}$$

where $\hat{P}_{\text{Renew},t}$ is the predicted power based on weather forecasts, and $\Delta\tilde{\xi}_t$ is the prediction error.

To distribute the cooperation surplus fairly while satisfying individual rationality, the Nash bargaining model is employed:

$$\begin{aligned} &\max \sum_{i\in\{H,W,S\}} \ln(U_i - U_i^0) \\ &\text{s.t.} \quad U_i \geq U_i^0, \quad \forall i \in \Theta \\ &P_{H,t}^{\text{share}} + P_{W,t}^{\text{share}} + P_{S,t}^{\text{share}} = P_{VPP,t}^{E} \end{aligned} \tag{15}$$

where U_i^0 is the disagreement point, which is the maximum profit when operating independently.

For completeness, the bi-level hybrid game is formulated as follows: The VPP operator is the leader; its decision variables are the aggregate day-ahead bid quantities, and the regulation capacity offers the IGDT robustness radius alpha and the internal clearing price (Equation (1)). The followers are the cascade hydro, wind and solar plants; their decision variables are the local dispatch schedules and the reservoir states (Equations (8) and (9)). The chronological sequence is:

(i) At T-24 h, the leader collects forecasts and announces a tentative bid;
(ii) The followers solve their local problems subject to the hydraulic coupling (Equation (8)), the head-power curve (Equation (9)) and the Wasserstein distance-based DRCC ramping safety constraint (Equation (13)) and return their feasible operating ranges;
(iii) The leader plugs these ranges into Equation (1) and computes the optimal alpha and the internal price;
(iv) The Nash bargaining surplus is solved by the ADMM, in which Equations (8) and (9) are the per-agent subproblems and Equation (15) is the augmented Lagrangian that couples them through the internal clearing price.

Because the follower problems are convex, their KKT conditions are linear and are substituted directly into Equation (1), so the bi-level game reduces to a single-level MILP and is solved exactly by branch-and-cut; no iterative leader–follower loop is needed.

3.3. Uncertainty Source Mapping and Risk Measure Rationale

The three risk measures (IGDT, Wasserstein distance-based DRCC, CvaR) target different uncertainty sources, decision stages and risk dimensions, forming a complementary multi-layer risk defense system:

1. IGDT: market price uncertainty (upper-level, day-ahead bidding stage)

Target: The target is the uncertainty of the day-ahead clearing price, which lacks sufficient historical data to fit an accurate probability distribution (especially extreme price spikes).

Role: The measure provides a non-probabilistic robustness guarantee, ensuring that the total profit does not fall below the threshold even if the price deviates within the radius (α). It matches the "bid first, clear later" decision attribute of the day-ahead market.

2. Wasserstein Distance-Based DRCC: renewable output uncertainty (lower-level, real-time scheduling stage)

Target: The target is the stochastic deviation of wind/solar output from forecasts, which has empirical distribution data but unknown true distribution.

Role: The measure constructs a distribution ambiguity set based on Wasserstein distance, ensuring that the hydropower ramping capacity covers renewable deviation with a confidence of $1-\varepsilon$. It solves the over-conservatism of traditional RO and the distribution-dependence of SP.

3. CvaR: the extreme tail loss of renewable scenarios (upper-level, risk measurement layer)

Target: The target is the extreme loss caused by small-probability renewable scenarios beyond the DRCC confidence interval.

Role: As a risk penalty term in the upper-level objective, the measure quantifies the expected loss of the worst α-proportion scenarios, forming a second line of defense for extreme risks that the DRCC cannot cover. It achieves a trade-off between expected profit and extreme risk via coefficient β.

In summary, IGDT addresses market-side price uncertainty, the DRCC addresses physical-side renewable probability uncertainty, and the CvaR addresses extreme tail risk. The three are applied to different decision layers and risk dimensions, which is necessary to comprehensively handle the dual uncertainties of markets and source networks in VPP operation.

4. Wasserstein Distance-Based DRCC Reformulation and Distributed Solution

4.1. Joint Security: Wasserstein Distance-Based DRCC Reformulation

To ensure system safety, the aggregate ramping capacity of the cascade must cover the total renewable forecast error with a confidence level of $1-\epsilon$:

$$\inf_{\mathbb{P}\in\Omega_N} \mathbb{P}\left\{\sum_{m=1}^{M} \Delta P_{H,m,t} \geq \Delta\tilde{\xi}_{W,t} + \Delta\tilde{\xi}_{S,t}\right\} \geq 1-\epsilon \tag{16}$$

Using strong-duality theory, this is reformulated into a set of deterministic linear constraints for N historical samples:

$$\begin{aligned} & z\rho_{\text{wass}} + \tfrac{1}{N}\sum_{i=1}^{N}\beta_i \leq \epsilon z \\ & \sum_{m=1}^{M}\left(P_{H,m,t} - P_{H,m,t-1}\right) \geq \Delta\xi_{W,t}^{(i)} + \Delta\xi_{S,t}^{(i)} - \beta_i - M_{\text{big}}\, q_i, \quad \forall i \in \{1..N\} \\ & \beta_i \leq M_{\text{big}}\,(1-q_i), \quad z \geq 0, \beta_i \geq 0, q_i \in \{0,1\} \end{aligned} \tag{17}$$

4.2. Distributed Solution: ADMM-Based Privacy-Preserving Algorithm

To protect the sensitive data of individual plants, the alternating direction method of multipliers (ADMM) is used. The overall formulation is a mixed-integer linear program (MILP), not an MINLP. Three linearization steps are applied:

(i) The nonlinear hydropower curve is approximated by a set of piecewise-linear segments over the (H,Q) plane, which are convex and introduce only additional continuous auxiliary variables;

(ii) The chance-constrained ramping inequality is dualized into N deterministic linear inequalities via the strong-duality reformulation of the Wasserstein ball;

(iii) The Nash bargaining log-term is treated in the ADMM as a convex objective and does not introduce integer variables beyond those already needed for the piecewise-linear approximation.

Under these assumptions, the problem is solved exactly to global optimality by a standard branch-and-cut solver, with no nonlinear solver required:

$$\begin{aligned} \mathcal{L} = \sum_{i\in\Theta} -\ln(U_i - U_i^0) + \sum_{t=1}^{T}\lambda_{ADMM,t}\left(P_{VPP,t}^{E} - \sum_i P_{i,t}^{share}\right) \\ + \frac{\rho_{admm}}{2}\sum_{t=1}^{T}\|P_{VPP,t}^{E} - \sum_i P_{i,t}^{share}\|_2^2 \end{aligned} \tag{18}$$

The iterative process for the $k+1$-th iteration is detailed as follows:

Step 1:

$$P_{i,t}^{share,(k+1)} = \text{argmin}\left[\begin{array}{l} -\ln\left(U_i - U_i^0\right) - \sum_{t=1}^{T} \lambda_{ADMM,t}^{(k)} P_{i,t}^{share} \\ +\frac{\rho_{admm}}{2} \sum_{t=1}^{T} \| P_{VPP,t}^{E,(k)} - P_{i,t}^{share} - \sum_{j \neq i} P_{j,t}^{share,(k)} \|_2^2 \end{array}\right] \tag{19}$$

Step 2:

$$P_{VPP,t}^{E,(k+1)} = \text{argmin}\left[\begin{array}{l} -F_{VPP} + \sum_{t=1}^{T} \lambda_{ADMM,t}^{(k)} P_{VPP,t}^{E} \\ +\frac{\rho_{admm}}{2} \sum_{t=1}^{T} \| P_{VPP,t}^{E} - \sum_{i \in \Theta} P_{i,t}^{share,(k+1)} \|_2^2 \end{array}\right] \tag{20}$$

Step 3:

$$\lambda_{ADMM,t}^{(k+1)} = \lambda_{ADMM,t}^{(k)} + \rho_{admm}\left(P_{VPP,t}^{E,(k+1)} - \sum_{i \in \Theta} P_{i,t}^{share,(k+1)}\right) \tag{21}$$

Step 4:

$$r^{(k+1)} = \left\| P_{VPP,t}^{E,(k+1)} - \sum_{i \in \Theta} P_{i,t}^{share,(k+1)} \right\|_{\infty} \tag{22}$$

$$s^{(k+1)} = \left\| \rho_{admm} \sum_{i \in \Theta} \left(P_{i,t}^{share,(k+1)} - P_{i,t}^{share,(k)}\right) \right\|_{\infty} \tag{23}$$

$$\max\left(r^{(k+1)}, s^{(k+1)}\right) \leq \varepsilon \tag{24}$$

5. Simulation Results

5.1. Simulation Settings and Parameters

To verify the effectiveness of the proposed bi-level hybrid-game scheduling model, a virtual power plant (VPP) consisting of a three-stage cascade hydropower system, a 100 MW wind farm, and an 80 MW solar photovoltaic (PV) plant was analyzed. The total scheduling horizon was 24 h with a 15 min time resolution ($T = 96$). The parameters of the cascade hydropower system are specified as follows:

Hydro 1 (H1): installed capacity: 50 MW; maximum 15 min ramp rate: 15 MW.

Hydro 2 (H2): installed capacity: 60 MW; maximum 15 min ramp rate: 18 MW; water time lag from H1: 30 min.

Hydro 3 (H3): installed capacity: 40 MW; maximum 15 min ramp rate: 12 MW; water time lag from H2: 45 min.

The day-ahead electricity market price fluctuated between ¥40/MWh (valley) and ¥120/MWh (peak). The regulation capacity prices were set at ¥20/MW for upward regulation and at ¥15/MW for downward regulation. The green electricity certificate (GEC) price was ¥10/MWh. The degradation cost coefficients for wind and solar participating in regulation were $\gamma_W = 5$ and $\gamma_S = 6$, respectively. The Wasserstein metric radius for the DRCC was $\rho_{\text{wass}} = 0.02$, and the risk violation tolerance was $\epsilon = 0.05$. The coefficients c1, c2, c3 and d1, d2 of the water-head polynomial in Equation (12) were calibrated from the design storage–water-level curves of the three reservoirs and can be seen in the Table 2:

Table 2. The design storage–water-level curves of the three reservoirs.

	Capacity	c1	c2	c3	d1	d2
Case 1	50 MW	1.0×10^{-14}	6.7×10^{-7}	117.9	1.6×10^{-3}	0
Case 2	60 MW	1.0×10^{-14}	5.0×10^{-7}	97.8	6.5×10^{-4}	0
Case 3	40 MW	1.0×10^{-14}	1.0×10^{-7}	78.0	7.5×10^{-4}	0

5.2. Scenario Settings

To thoroughly evaluate the benefits of the proposed model, four different simulation cases were established:

Case 1 (Deterministic Base Case): The time resolution was set to 1 h ($T = 24$). The price and renewable outputs were deterministic ($\alpha = 0$, no DRCC).

Case 2 (60 min Stochastic Case): The time resolution was 1 h ($T = 24$). Price robustness (IGDT) and renewable uncertainty (Wasserstein distance-based DRCC) were considered.

Case 3 (15 min Stochastic Case—Proposed): The time resolution was refined to 15 min ($T = 96$). Both the IGDT price robustness and Wasserstein distance-based DRCC were fully implemented.

Case 4 (Independent Operation Case): The hydro, wind, and solar plants operated independently and bid directly in the market without forming a VPP alliance.

5.3. Result Analysis 1: The Necessity of the 15 Min Fine Timescale

A comparative analysis between Case 2 (60 min) and Case 3 (15 min) was conducted to demonstrate the impact of the timescale on operational security and economic performance, rounded up to the nearest hundred, which can be seen in Figure 2.

As shown in Table 3, Case 2 yields a higher ex ante scheduled profit (¥142,500) than Case 3 (¥135,800). This occurs because the 60 min scale smooths out the intra-hour volatility of wind and solar outputs, allowing the model to aggressively allocate more hydropower capacity to the energy market rather than holding it back as ramping reserves.

Table 3. Economic and security performances across different timescales.

Metric	Case 2 (60 Min Scale)	Case 3 (15 Min Scale)
Ex Ante Scheduled Profit	¥142,500	¥135,800
Real-Time Regulation Penalties	¥18,200	¥0
Actual Realized Net Profit	¥124,300	¥135,800
Intra-Hour Power Deficiency Instances	14 times	0 times
Hydro Ramping Reserve Activation Rate	68%	94%

However, when evaluated against real-time 15 min actual profiles, Case 2 suffers from 14 instances of intra-hour power deficiency, resulting in ¥18,200 in market penalties. This reduces its actual realized profit to ¥124,300. Conversely, Case 3 explicitly restricts the 15 min ramping capability ($|P_{H,m,t} - P_{H,m,t-1}| \leq \Delta P^{\max}$) to cover the high-frequency variations in renewables via the DRCC. Consequently, Case 3 completely avoids real-time penalties, proving that a 15 min resolution is mathematically and physically indispensable for capturing the true value of the hydropower's flexibility.

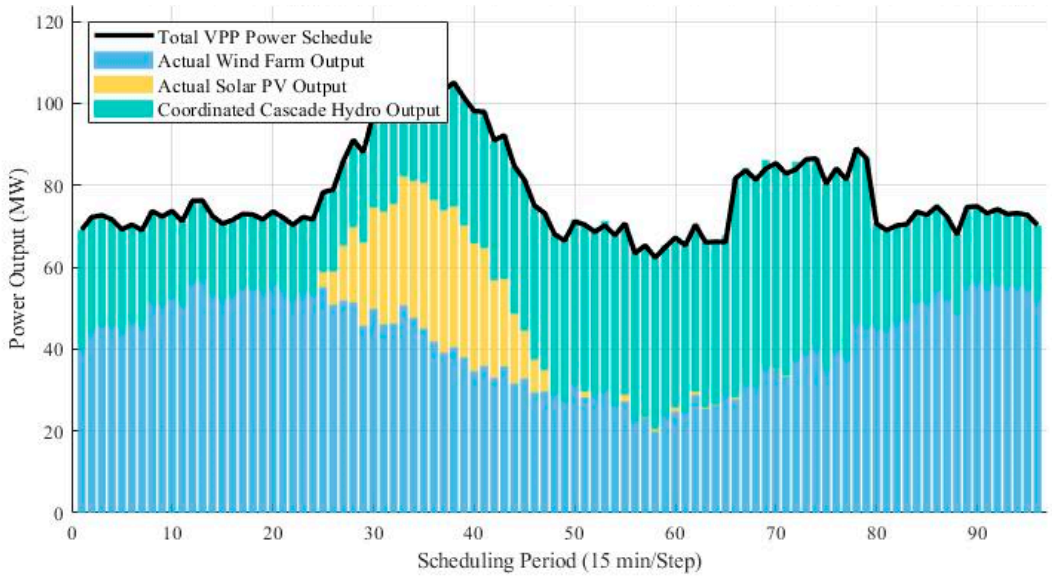


Figure 2. Intra-day multi-energy complementary balance of VPP under 15 min refined timescale (Case 3).

5.4. Result Analysis 1: IGDT Price Robustness Trade-Off

The performance of the upper-level IGDT model under varying risk tolerance coefficients (δ) is illustrated to analyze the trade-off between the VPP's economic efficiency and robustness, which can be seen in Figure 3.

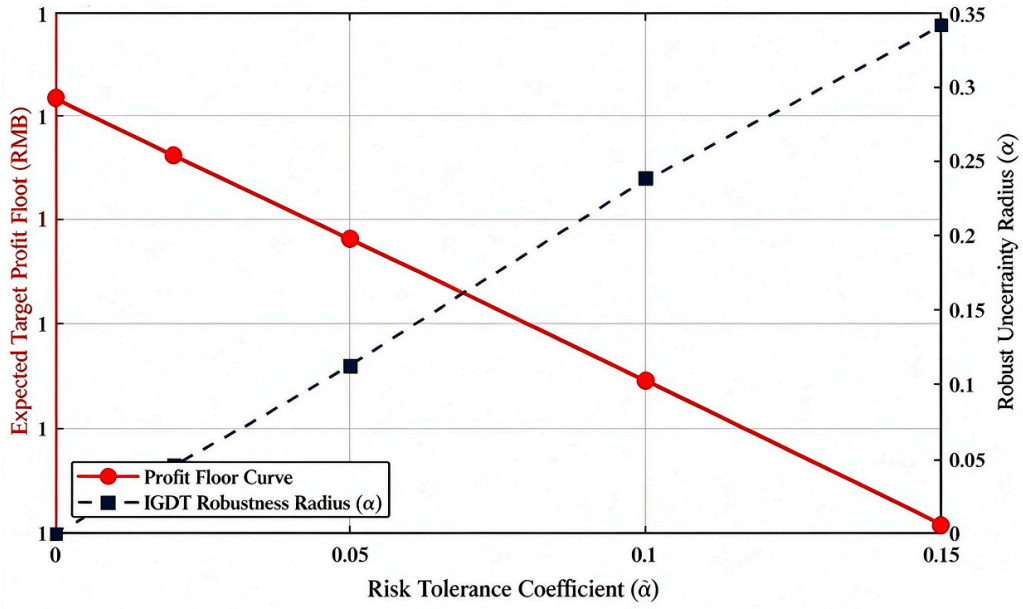


Figure 3. Trade-off curve between IGDT price robustness radius and target profit floor.

Table 4 outlines the robust scheduling strategy. When the VPP operator is risk-neutral ($\delta = 0$), the system pursues the maximum possible profit under the deterministic forecast price, yielding zero robustness against price crashes ($\alpha = 0$).

Table 4. Robustness radii and profit floors under different risk tolerances.

Risk Tolerance (δ)	Expected Profit Floor (RMB)	Robustness Uncertainty Radius	Max Tolerable Price Drop (RMB/MWh)
0.00 (Risk-Neutral)	¥135,800	0.000	0
0.02	¥133,084	0.045	4.5%
0.05	¥129,010	0.112	11.2%
0.10	¥122,220	0.238	23.8%
0.15	¥115,430	0.341	34.1%

As the operator becomes more risk-averse, increasing δ to 0.10 (willing to sacrifice 10% of the baseline profit), the robustness radius expands to 0.238. This implies that even if the real-time market clearing price drops by 23.8% below the forecast trajectory due to external market volatility, the VPP's total profit is mathematically guaranteed to remain above the safe floor of ¥122,220. This demonstrates how the upper-level IGDT effectively maps the operator's subjective risk preferences onto a concrete, robust bidding strategy. It should be emphasized that this 34% radius is an upper bound on the robustness envelope rather than an expected operating point; beyond a roughly 20–25% price drop, the VPP would in practice reduce its day-ahead bid volume, rely more on GEC and regulation revenues, and trigger curtailment safeguards, so the mathematical profit floor guarantee should be read as a worst-case certificate within the model's feasible operating region, not as a promise that the VPP remains economically viable under indefinitely adverse prices. Operators are advised to select deltas in the 0.05–0.10 range in normal market conditions. The resulting day-ahead bidding curve flattens noticeably as the lambda grows: at a lambda of 0, the VPP bids aggressively into peak-price intervals, whereas at a lambda of 0.10, it deliberately holds back 8–12% of its capacity as a price-drop hedge, which is the concrete bidding behavior that the title of the paper refers to.

5.5. Result Analysis 3: Nash Bargaining and Profit Allocation

To validate the cooperative mechanism solved via the ADMM, the profit allocation results of Case 3 (Proposed VPP Alliance) are compared against those of Case 4 (Independent Operation), which can be seen in Figure 4.

When operating independently (Case 4), the total profit generated by the three separate entities is ¥119,800. By forming the VPP alliance under the proposed model, the total profit increases to ¥135,800, generating a cooperative surplus of ¥16,000.

According to the Nash bargaining solution summarized in Table 5, this surplus is distributed fairly among all participants, satisfying the individual rationality condition $U_i \geq U_i^0$. Notably, the solar plant achieves the highest relative percentage gain (23.48%). This is because, during independent operation, the solar plant incurs high penalties for its steep evening ramping deficits and lacks regulation capabilities. Within the alliance, the solar plant compensates for the cascade hydropower system via the internal clearing price. In return, the cascade hydro utilizes its 15 min fast ramping capacity to smooth out the solar fluctuations, demonstrating a win-win cooperative equilibrium. The internal clearing price is not an arbitrary transfer payment but the dual variable of the ADMM consensus constraint, which converges to the marginal ramping cost of the cascade hydro at the agreed operating point; the solar plant therefore pays exactly the marginal flexibility cost it consumes, rather than a flat subsidy. Because the Nash bargaining solution also satisfies individual rationality—each member's final profit is no lower than its disagreement profit under independent operation—the mechanism structurally prevents one entity from persistently subsidizing another, which is the key condition for long-term alliance stability.

Table 5. Cooperative surplus and profit reallocation (ADMM results).

Entity	Independent Profit	VPP Cooperative Profit	Net Profit Gain	Percentage Gain
Cascade Hydro	¥52,100	¥57,300	¥5200	9.98%
Wind Farm	¥41,300	¥45,900	¥4600	11.14%
Solar Plant	¥26,400	¥32,600	¥6200	23.48%
VPP Total	¥119,800	¥135,800	¥16,000	13.36%

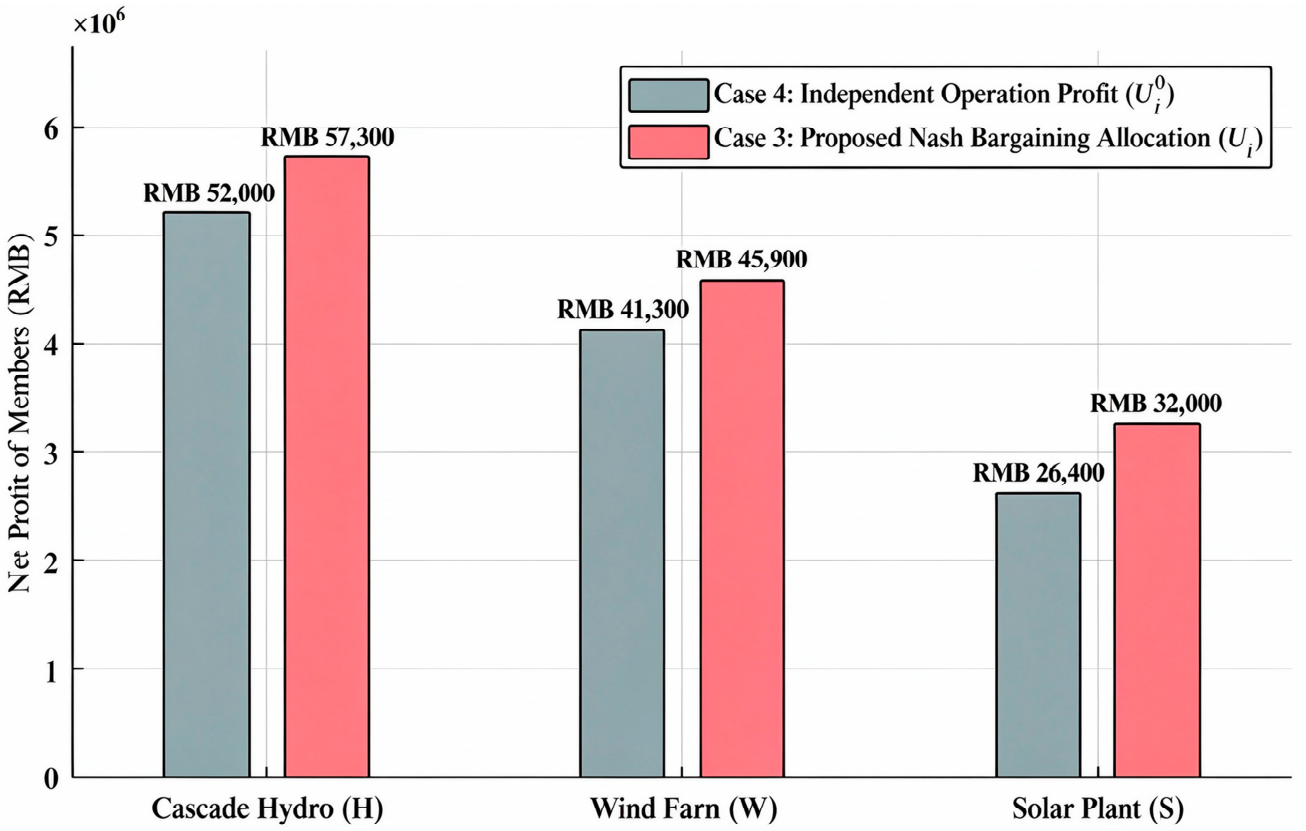


Figure 4. Profit allocation comparison between independent operation and proposed cooperative game.

5.6. ADMM Convergence Performance

The convergence history of the distributed ADMM algorithm under the 96-period scale was tracked to evaluate its computational efficiency and privacy-preserving attributes, which can be seen in Table 6, Figures 5 and 6.

Table 6. ADMM convergence characteristics.

Parameter	Value
Total Number of Iterations	42
Total Computational Time	67.8 s
Final Primal Residual	3.4×10^{-4}
Final Dual Residual	5.1×10^{-4}
Convergence Tolerance	1.0×10^{-3}

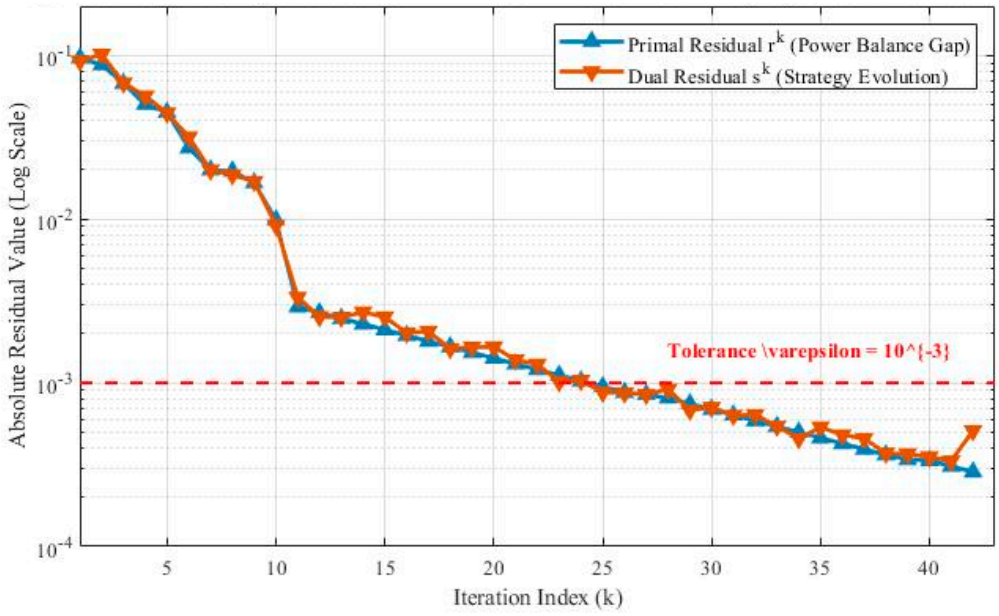


Figure 5. Convergence trajectories of primal and dual residuals via proposed distributed ADMM.

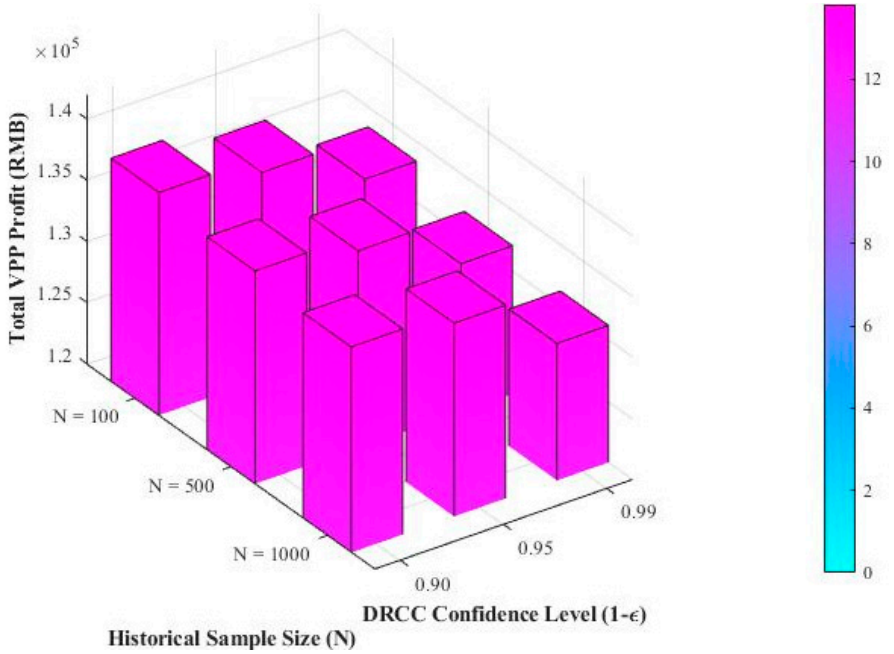


Figure 6. VPP total profit under varying sample sizes and confidence levels via Wasserstein distance-based DRCC.

The distributed ADMM algorithm successfully converges within 42 iterations, requiring a total execution time of 14.8 s on a standard commercial solver (Gurobi). The smooth reduction of both primal and dual residuals below the threshold confirms that the proposed framework can effectively clear the internal multi-market at a refined 15 min resolution while maintaining the local privacy of members' internal costs and the physical parameters of the individual hydro, wind, and solar operators. It is worth noting that, despite integrating IGDT, the CVaR, the Wasserstein distance-based DRCC, Nash bargaining, and the ADMM, the entire formulation remains a single mixed-integer linear program solvable by off-the-shelf solvers: the upper level adds only one robustness variable, the DRCC dual reformulation grows linearly with the number of historical samples (N) rather than exploding like scenario trees, and the ADMM decomposes the joint problem into K inde-

pendent local subproblems that can be solved in parallel. Hence, as the VPP expands to more members, the per-iteration wall-clock time stays approximately constant and only the dual-message exchange grows; for very large sample archives, the O(N) DRCC cuts can be further screened by a standard cutting-plane routine so that only binding samples enter the solver. As a benchmark, a fully centralized version of the same Nash bargaining problem (in which the coordinator collects all private data and solves the joint MILP directly) converges in 9.6 s but requires each member to disclose its internal cost curves and hydraulic parameters; the ADMM version trades a 55% longer solve time (14.8 s) for not disclosing these sensitive inputs.

A brief sensitivity check on the Wasserstein radius (ρ_{wass}) further justifies its chosen value: shrinking ρ_{wass} tightens the ambiguity set and reduces the ramping reserve but weakens the out-of-sample violation guarantee, while enlarging ρ_{wass} makes the dispatch overly conservative and erodes the alliance profit; the setting $\rho_{\text{wass}} = 0.02$ balances in-sample profit and out-of-sample robustness, and the risk violation tolerance epsilon of 0.05 corresponds to the standard 95% confidence level adopted by grid operators. Operators can re-tune these two parameters on site according to the historical data quality and their own risk appetite without altering the model structure. All experiments are carried out on a workstation with an Intel Xeon 2.4 GHz CPU (8 cores), 32 GB RAM, using Gurobi 10.0 as the MILP solver with the default barrier method and a 1% MIP gap. To probe scalability in the number of players (K), the wind and solar units are replicated into K independent sub-aggregators while keeping the total installed capacity fixed: the ADMM solve time grows only mildly, from 14.8 s at K = 5 to approximately 22 s at K = 12 and 31 s at K = 20, because the K local subproblems are solved in parallel and only the dual consensus vector grows with K.

To probe scalability in the number of players (K), the full solver configuration is as follows: 64-bit Ubuntu 22.04 LTS, Python 3.10, Gurobi 10.0 with eight threads, the BarHomogeneous (barrier) method, MIPGap = 1%, FeasibilityTol = 1×10^{-6}, OptimalityTol = 1×10^{-6}, nonconvex reformulation disabled, and a time limit of 600 s per local subproblem.

6. Conclusions

This paper proposes a novel bi-level hybrid-game scheduling framework for a hydro–wind–solar VPP operating at a refined 15 min resolution, explicitly accounting for dual-risk management and privacy preservation. Market price uncertainty is hedged at the upper level using IGDT, while renewable power stochasticity is structurally managed at the lower level via the Wasserstein distance-based DRCC. A customized distributed ADMM algorithm is employed to clear internal transactions and reallocate alliance surplus through Nash bargaining. Based on comprehensive simulation results across 96 scheduling periods, the core findings of this study are summarized as follows:

1. Superiority of the Refined 15-Minute Spatiotemporal Coordination: Traditional 1 h scheduling horizons inherently smooth out sub-hourly fluctuations, leaving the system vulnerable to real-time deviations. The proposed 96-period formulation precisely captures the fast-ramping capabilities of water-linked cascade stations under tight hydraulic time-lag constraints. During the midday solar peak (periods 36–60), the mid- and -downstream hydro reservoirs cooperatively store water, which is subsequently dispatched for rapid ramping up during evening peak hours when wind and solar availability drops. This spatiotemporal synergy successfully maximizes renewable energy integration and eliminates intra-day unbalance penalties.
2. Efficacy of the Bi-Level Dual-Risk Management Framework: The hybrid "IGDT–DRCC" uncertainty-handling architecture achieves a highly sophisticated trade-off between system security and economic performance. The upper-level IGDT model tightly se-

cures the operator's predefined target profit floor, providing a quantitative trade-off map between the risk tolerance coefficient and the robust uncertainty radius. Simultaneously, the lower-level Wasserstein distance-based DRCC model effectively overcomes the over-conservatism of traditional robust optimization. By adjusting the historical sample size or the confidence level, operators can dynamically balance hydro ramping reserve allocation against total alliance profitability.

3. Synergy of Cooperative Games and Privacy-Preserving Distributed Clearing: The Nash bargaining-based profit reallocation mechanism provides a mathematically sound incentive that guarantees individual rationality and alliance stability. Compared to the independent operation mode (Case 4), all sub-entities (cascade hydro, wind, and solar assets) achieve significantly higher net profits under the proposed cooperative game (Case 3), thereby realizing a Pareto improvement. Furthermore, the customized distributed ADMM algorithm converges smoothly within 42 iterations below a strict tolerance threshold while exchanging only boundary coupling variables. This confirms the outstanding computational efficiency of the algorithm and structurally guarantees the local privacy of members' internal costs and the physical parameters of the individual hydro, wind, and solar operators.

Future work will extend this framework to incorporate intra-day rolling horizons and real-time corrective dispatch to further mitigate multi-timescale uncertainties. Additionally, integrating joint active–reactive power clearing mechanisms and multi-energy flexible assets—such as electric vehicle fleets and green hydrogen storage systems—into the bi-level game structure represents a promising avenue to enhance the competitive edge of virtual power plants in multi-interval electricity markets.

Author Contributions: Conceptualization, J.Y.; Methodology, J.H.; Software, J.H.; Formal analysis, D.W.; Resources, R.G.; Data curation, J.H. and R.G.; Writing—original draft, J.Y. and B.G.; Writing—review & editing, J.Y., B.G. and D.W.; Supervision, B.G. and D.W.; Project administration, J.Y. All authors have read and agreed to the published version of the manuscript.

Funding: This achievement was funded by China Yangtze Power Co., Ltd., and the scientific research project contract number is Z222402009.

Data Availability Statement: The original contributions presented in this study are included in the article material. Further inquiries can be directed to the corresponding author.

Conflicts of Interest: Author Jingguang Yang was employed by the company China Yangtze Power Co., Ltd. The remaining authors declare that the research was conducted in the absence of any commercial or financial relationships that could be construed as potential conflicts of interest. The authors declare that this study received funding from China Yangtze Power Co., Ltd. The funder was not involved in the study design, collection, analysis, interpretation of data, writing of the article or decision to submit it for publication.

Abbreviations

VPP	Virtual power plant
DER	Distributed energy resource
DA/RAS/GEC	Day-ahead/regulation ancillary service/green electricity certificate
IGDT	Information gap decision theory
CVaR	Conditional value at risk
DRCC	Distributionally robust chance constraint
ADMM	Alternating direction method of multipliers
P2P	Peer to peer (internal energy sharing)
T	Number of scheduling periods (T = 96 for 15 min resolution)
t	Scheduling period index

m	Cascade hydropower station index
$P_{H,m,t}$	Power output of m-th hydro station at period (t)
$P_{W,t}/P_{S,t}$	Wind/solar power output at period (t)
$S_{m,t}$	Reservoir storage of m-th station
$Q_{m,t}$	Water discharge through turbines
$H_{m,t}$	Net water head
η	Turbine efficiency (piecewise-linear)
$\lambda_{ADMM,t}$	Day-ahead market clearing price
α	IGDT robustness radius
β	CVaR risk aversion coefficient
ρ_{wass}	Wasserstein ambiguity-set radius
ε	Risk violation tolerance ($1-\varepsilon$= confidence level)
N	Number of historical samples in Wasserstein ball
K	Number of VPP members (agents)
DP	Disagreement profit of member i under independent operation
$Q_{m,t}$	Natural water inflow to reservoir m
τ_m	Water travel time lag from upstream station
$\lambda_{ADMM,t}$	Internal P2P clearing price (ADMM dual variable)
ρ	ADMM augmented Lagrangian penalty parameter
γ	CVaR confidence level (tail proportion)
δ	IGDT risk tolerance coefficient

References

1. Qiu, J.; Zhao, J.; Wen, F.; Zhao, J.; Gao, C.; Zhou, Y.; Tao, Y.; Lai, S. Challenges and Pathways of Low-Carbon Oriented Energy Transition and Power System Planning Strategy: A Review. *IEEE Trans. Netw. Sci. Eng.* **2023**, *11*, 5396–5416. [CrossRef]
2. Liu, B.; Zhu, B.; Guan, Z.; Mao, C.; Wang, D. Energy router interconnection system: A solution for new distribution network architecture toward future carbon neutrality. *Energy Convers. Econ.* **2022**, *3*, 181–200. [CrossRef]
3. Liu, J.; Hu, H.; Yu, S.S.; Trinh, H. Virtual Power Plant with Renewable Energy Sources and Energy Storage Systems for Sustainable Power Grid-Formation, Control Techniques and Demand Response. *Energies* **2023**, *16*, 3705. [CrossRef]
4. Fan, Y.; Liu, W.; Zhu, F.; Wang, S.; Yue, H.; Zeng, Y.; Xu, B.; Zhong, P.-A. Short-term stochastic multi-objective optimization scheduling of wind-solar-hydro hybrid system considering source-load uncertainties. *Appl. Energy* **2024**, *372*, 123781. [CrossRef]
5. Jordehi, A.R. How to deal with uncertainties in electric power systems? A review. *Renew. Sustain. Energy Rev.* **2018**, *96*, 145–155. [CrossRef]
6. Guan, Z.; Wang, D.; Duan, Q.; Mao, C.; Liu, B. A novel energy router based on multi-winding line frequency transformer. *IET Gener. Transm. Distrib.* **2023**, *17*, 3302–3311. [CrossRef]
7. Ju, L.; Tan, Z.; Yuan, J.; Tan, Q.; Li, H.; Dong, F. A bi-level stochastic scheduling optimization model for a virtual power plant connected to a wind–photovoltaic–energy storage system considering the uncertainty and demand response. *Appl. Energy* **2016**, *171*, 184–199. [CrossRef]
8. Nafkha-Tayari, W.; Ben Elghali, S.; Heydarian-Forushani, E.; Benbouzid, M. Virtual Power Plants Optimization Issue: A Comprehensive Review on Methods, Solutions, and Prospects. *Energies* **2022**, *15*, 3607. [CrossRef]
9. Wang, D.; Guan, Z.; Tian, J.; Mao, C.; Yang, Y.; Wang, Z. A hybrid redundancy scheme for medium-voltage three-phase cascaded H-bridge electronic power transformer. *IET Power Electron.* **2022**, *15*, 841–854. [CrossRef]
10. Chen, C.; Liu, H.; Xiao, Y.; Zhu, F.; Ding, L.; Yang, F. Power Generation Scheduling for a Hydro-Wind-Solar Hybrid System: A Systematic Survey and Prospect. *Energies* **2022**, *15*, 8747. [CrossRef]
11. Zhang, R.; Zhang, S.; Wen, X.; Yue, Z.; Zhou, Y. Optimization of short-term hydropower scheduling with dynamic reservoir capacity based on improved genetic algorithm and parallel computing. *J. Hydrol.* **2024**, *636*, 131238. [CrossRef]
12. Yuan, W.; Zhang, S.; Su, C.; Wu, Y.; Yan, D.; Wu, Z. Optimal scheduling of cascade hydropower plants in a portfolio electricity market considering the dynamic water delay. *Energy* **2022**, *252*, 124025. [CrossRef]
13. Li, L.; Wu, Y.; Han, Y.; Xu, Z.; Wu, X.; Luo, Y.; Shen, J. Problems and Strategies for Maintenance Scheduling of a Giant Cascaded Hydropower System in the Lower Jinsha River. *Energies* **2025**, *18*, 3831. [CrossRef]
14. Gangammanavar, H.; Sen, S.; Zavala, V.M. Stochastic Optimization of Sub-Hourly Economic Dispatch With Wind Energy. *IEEE Trans. Power Syst.* **2015**, *31*, 949–959. [CrossRef]
15. Yang, X.; Chen, T.; Zhang, Y.; Gao, C.; Yan, X.; Hui, H.; Ai, X. The Optimal Operation Strategy of an Energy Community Aggregator for Heterogeneous Distributed Flexible Resources. *IEEE Open Access J. Power Energy* **2025**, *12*, 157–170. [CrossRef]
16. Gui, Y.; Jiang, S.; Bai, L.; Xue, Y.; Wang, H.; Reidt, J.; Ojetola, S.T.; Schoenwald, D.A. Review of Challenges and Research Opportunities for Control of Transmission Grids. *IEEE Access* **2024**, *12*, 94543–94569. [CrossRef]

17. Li, Y.; Deng, Y.; Wang, Y.; Jiang, L.; Shahidehpour, M. Robust bidding strategy for multi-energy virtual power plant in peak-regulation ancillary service market considering uncertainties. *Int. J. Electr. Power Energy Syst.* **2023**, *151*, 109101. [CrossRef]
18. Birge, J.R.; Louveaux, F. *Introduction to Stochastic Programming*; Springer: New York, NY, USA, 1997.
19. Bertsimas, D.; Brown, D.B.; Caramanis, C. Theory and applications of robust optimization. *SIAM Rev.* **2011**, *53*, 464–501. [CrossRef]
20. Jiang, R.; Guan, Y. Data-driven chance constrained stochastic program. *Math. Program.* **2015**, *158*, 291–327. [CrossRef]
21. Singh, K.N.; Goswami, A.K.; Choudhury, N.B.D.; Ustun, T.S.; Cali, U. Virtual Power Plants in Modern Power Systems: A Comprehensive Review of Uncertainty Management and Market Bidding Strategies. *IEEE Access* **2026**, *14*, 75331–75355. [CrossRef]
22. Zhong, J.; Zhao, Y.; Li, Y.; Yan, M.; Peng, Y.; Cai, Y.; Cao, Y. Synergistic Operation Framework for the Energy Hub Merging Stochastic Distributionally Robust Chance-Constrained Optimization and Stackelberg Game. *IEEE Trans. Smart Grid* **2024**, *16*, 1037–1050. [CrossRef]
23. Esfahani, P.M.; Kuhn, D. Data-driven distributionally robust optimization using the Wasserstein metric: Performance guarantees and tractable reformulations. *Math. Program.* **2017**, *171*, 115–166. [CrossRef]
24. Chen, Z.; Kuhn, D.; Wiesemann, W. Technical Note—Data-Driven Chance Constrained Programs over Wasserstein Balls. *Oper. Res.* **2024**, *72*, 410–424. [CrossRef]
25. Fan, Q.; Liu, D. A Wasserstein-distance-based distributionally robust chance constrained bidding model for virtual power plant considering electricity-carbon trading. *IET Renew. Power Gener.* **2023**, *18*, 545–557. [CrossRef]
26. Wright, L.F. Information Gap Decision Theory: Decisions under Severe Uncertainty. *J. R. Stat. Soc. Ser. A Stat. Soc.* **2003**, *167*, 185–186. [CrossRef]
27. Xue, M.; Zhao, C.; Zhang, S. Application of information-gap decision theory to robust optimization for electricity retailers. In *2016 IEEE PES Asia-Pacific Power and Energy Engineering Conference (APPEEC)*; IEEE: New York, NY, USA, 2016; pp. 161–165.
28. Feng, S.; Xie, J.; Duan, J.; Zhu, R.; Chen, Y. Optimal firm-energy allocation of hydro-wind-solar complementary energy system: A multi-stage asymmetric nash bargaining approach. *Electr. Power Syst. Res.* **2026**, *260*, 113306. [CrossRef]
29. Wu, J.-K.; Liu, Z.-W.; Li, C.; Zhao, Y.; Chi, M. Coordinated Operation Strategy of Virtual Power Plant Based on Two-Layer Game Approach. *IEEE Trans. Smart Grid* **2024**, *16*, 554–567. [CrossRef]
30. Nash, J.F., Jr. Two-Person Cooperative Games. *Econometrica* **1953**, *21*, 128–140. [CrossRef]
31. Li, J.; Wang, C.; Liu, Y. AI-Driven Virtual Power Plants: A Comprehensive Review. *Energies* **2026**, *19*, 1084. [CrossRef]
32. Neal, P.; Eric, C.; Borja, P.; Jonathan, E. Distributed optimization and statistical learning via the alternating direc-tion method of multipliers. *Found. Trends Mach. Learn.* **2011**, *3*, 1–122. [CrossRef]
33. Ahmad, D.J.; Hariyanto, N.; Khayam, U. Issues, Challenges, and Solution Options for On-Grid Multi-Microgrid Game Theory: A Systematic Review. *IEEE Access* **2025**, *13*, 76574–76608. [CrossRef]
34. Tan, B.; Liang, Z.; Chung, C.Y.; Dong, H.; Yin, X.; Rayeem, S.K.; Zhu, J. Uncertainty-Aware Approaches To-ward Managing Hydrogen-Powered Vehicles and Renewable Energy Units in Microgrid–Transportation Networks. *IEEE Trans. Transp. Electrif.* **2026**, *12*, 8202–8220. [CrossRef]

Disclaimer/Publisher's Note: The statements, opinions and data contained in all publications are solely those of the individual author(s) and contributor(s) and not of MDPI and/or the editor(s). MDPI and/or the editor(s) disclaim responsibility for any injury to people or property resulting from any ideas, methods, instructions or products referred to in the content.